

CORONAL MASS EJECTIONS AND SOLAR POLARITY REVERSAL

N. GOPALSWAMY

NASA/Goddard Space Flight Center, Greenbelt, MD 20771; gopals@fugee.gsfc.nasa.gov

A. LARA¹ AND S. YASHIRO

Department of Physics, Catholic University of America, 200 Hannan Hall, Washington, DC 20064

AND

R. A. HOWARD

Naval Research Laboratory, 4555 Overlook Avenue Southwest, Washington, DC 20375

Received 2003 September 10; accepted 2003 October 6; published 2003 October 31

ABSTRACT

We report on a close relationship between the solar polarity reversal and the cessation of high-latitude coronal mass ejections (CMEs). This result holds good for individual poles of the Sun for cycles 21 and 23, for which CME data are available. The high-latitude CMEs provide a natural explanation for the disappearance of the polar crown filaments (PCFs) that rush the poles. The PCFs, which are closed field structures, need to be removed before the poles could acquire open field structure of the opposite polarity. Inclusion of CMEs along with the photospheric and subphotospheric processes completes the full set of phenomena to be explained by any solar dynamo theory.

Subject headings: Sun: activity — Sun: coronal mass ejections (CMEs) — Sun: magnetic fields — Sun: prominences

1. INTRODUCTION

Common signatures of magnetic polar reversals on the Sun are the disappearance and reformation of polar coronal holes (Webb, Davis, & McIntosh 1984; Bilenko 2002; Harvey & Recely 2002) and the disappearance of the polar crown filaments (PCFs) following a sustained march to the poles (Waldmeier 1960; Makarov, Tlatov, & Sivaraman 2001). These signatures are, of course, related: during the interval between the disappearance of the old-polarity coronal hole and the reformation of the new-polarity coronal hole, the PCFs that approach the poles need to disappear. Filaments/prominences do not occur naked but have overlying closed field structures, commonly known as helmet streamers. Thus, we would expect the complete disappearance of these closed field structures when the polarity changes. Prominence disappearances are known to be either eruptive or thermic (see, e.g., Wagner 1986). Only eruptive prominences can be relevant, because thermic disappearances represent a temporary heating of the prominence. Gopalswamy et al. (2003a) noted that prominence eruptions at high latitudes subsided around the time of the polarity reversals. Since eruptive prominences are almost always accompanied by coronal mass ejections (CMEs), one can identify the disappearance of PCFs with high-latitude (HL) CMEs (Gopalswamy et al. 2003b). Thus CMEs may be intimately connected to the mechanism of polarity reversal. We test this possibility using the well-observed CMEs of solar cycles 23 and 21.

2. ANALYSIS AND RESULTS

The primary CME data needed for this study were obtained by the *Solar and Heliospheric Observatory (SOHO)* mission's Large Angle and Spectrometric Coronagraph Experiment (LASCO; Brueckner et al. 1995) for cycle 23. The CME rates for 1996–2002 were derived from the online catalog.² There were no spaceborne coronagraphs operating during the polarity-reversal times of solar cycle 22. For cycle 21, the CMEs were

observed by the Solwind coronagraph on board the *P78-1* satellite (Cliver et al. 1994).³ We use the National Solar Observatory's Kitt Peak magnetograph measurements available online to track the evolution of the photospheric magnetic field strength in the polar regions and identify the epochs of polarity reversal. We extend the list of prominence eruptions from the Nobeyama radioheliograph studied by Gopalswamy et al. (2003b) to include events from 2002.

2.1. Prominence Eruptions and CMEs

In a recent paper, Gopalswamy et al. (2003b) established that prominence eruptions (PEs) and CMEs are closely related and had similar latitude dependence. Figure 1 compares the latitudinal distribution of PEs and CMEs along with the tilt angle (maximum excursions of the heliospheric current sheet as available from the Wilcox Solar Observatory Web site⁴). We note the close similarity between the PE and CME distributions at various latitudes. Of particular importance for this Letter is the north-south asymmetry in the HL activities. The epochs when the HL PEs and CMEs subside (marked by the vertical lines) are clearly different in the north and south. Nobeyama radioheliograph observes the Sun only for 8 hr day⁻¹ and only limb events are automatically detected, so the sample size is relatively small. We show that the epochs of cessation of HL PEs also mark when the general population of HL CMEs subsides.

2.2. CME Occurrence Rate

Figure 2 shows the occurrence rate of LASCO CMEs averaged over Carrington rotation (CR) periods. The error bars are computed based on *SOHO* down times during each rotation (Gopalswamy et al. 2003c). Also shown are the daily sunspot numbers (SSNs). Although there is an overall similarity between the SSN and the CME rates, there are clear differences in detail. The CME rate peaks in 2002, roughly 2 yr after the peak in the SSN. The sunspot activity is confined to the active

¹ On leave from the Instituto de Geofísica, UNAM, Mexico.

² See http://cdaw.gsfc.nasa.gov/CME_list.

³ As listed in http://lasco-www.nrl.navy.mil/solwind_transient.list.

⁴ See <http://http://quake.stanford.edu/wso/Tilts.html>.

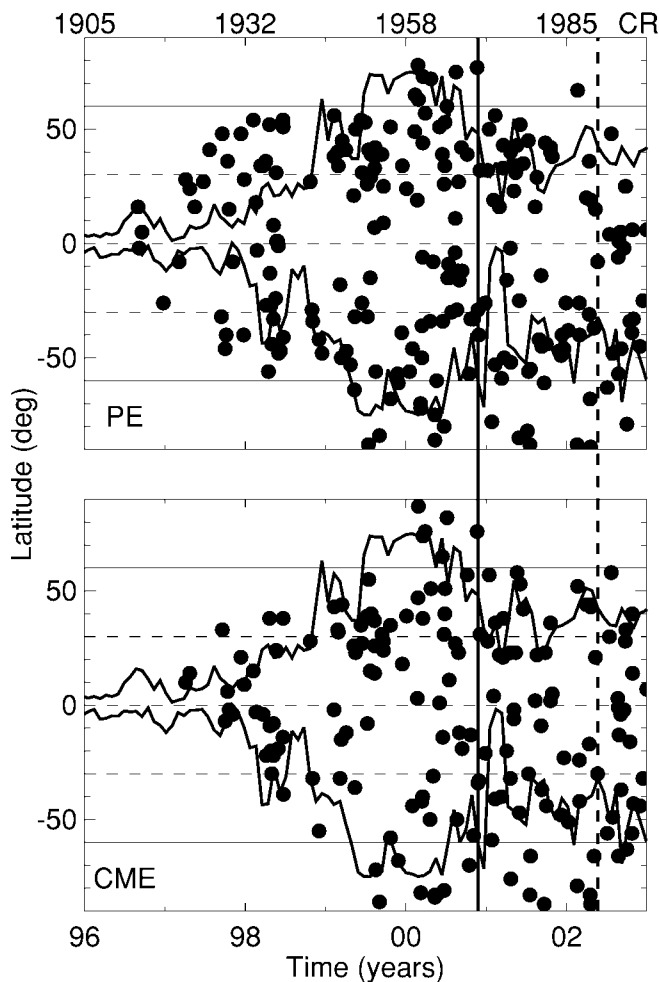


FIG. 1.—*Top*: Latitude distribution of all the prominence eruptions detected by the Nobeyama radioheliograph as a function of time from 1996 to 2002 (the CR numbers are marked at the top). The 60° latitude is shown as a solid line to show the HL eruptions. The solid curves in the northern and southern hemispheres represent the maximum excursions of the heliospheric current sheet, a good indicator of the presence of neutral lines at high latitudes. The vertical lines (*solid*: north; *dashed*: south) show the epochs of cessation of HL activity. The overall ratio of HL and LL CMEs is 16%. *Bottom*: Same as above, but for the associated CMEs.

region belt (low to mid latitudes), but the CME activity occurs at all latitudes. Separating HL and low-latitude (LL) CMEs thus provides a convenient way of grouping sunspot-related and PCF-related CMEs. The CME latitudes can be obtained by converting the observed central position angle to the latitude of the CMEs. It is likely that some LL CMEs may be misidentified as HL CMEs because of projection effects. To minimize this, we have grouped CMEs with apparent latitude $\leq 40^\circ$ as LL CMEs and those with latitude $\geq 60^\circ$ as HL CMEs. The rates of LL and HL CMEs are also shown in Figure 2. The overall ratio of HL to LL rates is 25% (20% when CMEs above and below 60° latitude are considered). Occasionally, the ratio was close to 100% during short intervals. The LL CME rate is remarkably flat during solar maximum (except for the fluctuations) compared to all the other rates. The HL CME rate displays more variability and is of interest for this study.

2.3. HL CME Rate and Polarity Reversal

The variation of the photospheric magnetic field of cycle 23, averaged over longitudes and poleward of 70° , is shown in

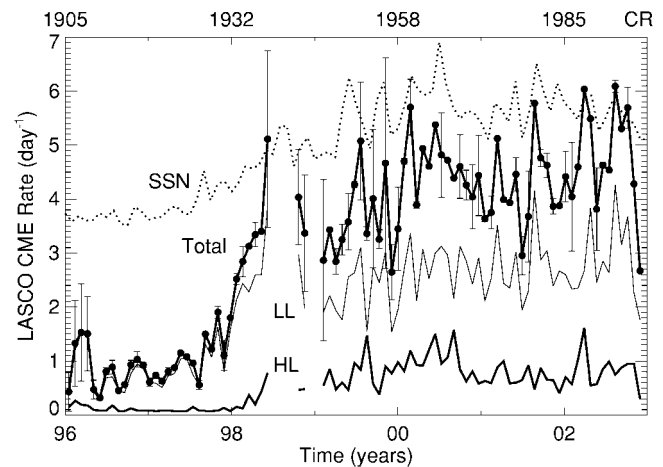


FIG. 2.—Occurrence rate of CMEs as obtained by the *SOHO*/LASCO coronagraphs (*solid line with filled circles*) compared with daily SSNs. CME rates corresponding to low ($\leq 40^\circ$) and high latitudes ($\geq 60^\circ$) are also shown and marked as LL and HL, respectively. There were 4607 LL CMEs and 1159 HL CMEs in the data set (excluding the CMEs from the 40° – 60° latitude range). All rates are averaged over CR periods. The CR numbers are indicated at the top. The breaks in the rate plots correspond to the two *SOHO* data gaps in 1998 June–October and 1999 January.

Figure 3. Starting in the middle of the year 1999, the field strengths at both poles decline and the first signs of reversal occur in early 2000. The reversal is obviously not a sharp process and is completed only after a few episodes of temporary reversals (marked by the vertical lines). The magnetic field strength displays an “unsettled behavior” during the years 2000–2002, with several short-duration reversals. In order to see how the HL CMEs are related to the polarity reversals in the individual hemispheres, we have separated the HL CME rate into northern (NHL) and southern (SHL) components (see Fig. 3, *middle panel*). We have also indicated the 3σ (standard deviation) rates by horizontal lines (*solid*: north; *dotted*: south) to assess the significance of the peaks. First of all, we note that there was a rapid increase in HL CMEs in the middle of the year 1999, especially in the northern hemisphere. After a local minimum, the NHL CME rate again had a broad maximum before dropping to a low value. On the basis of the magnetic field data, the north polar reversal was reported to be in 2001 February (Bilenko 2002) and 2001 May (Durrant & Wilson 2003). Figure 3 shows that the north polar field strength was close to zero at these times. In 2000 October there was a definite reversal (*thick line*), which coincided with the times of PCF disappearance (Lorenc, Pasorek, & Rybanský 2003; Harvey & Recely 2002; Gopalswamy et al. 2003a). The SHL CME activity picked up around the same time as the NHL CMEs, but the activity continued beyond the year 2002, subsiding after a large peak in the first half of 2002. The south polar reversal was reported to be in 2001 September (Durrant & Wilson 2003) and 2002 January (Bilenko 2002), consistent with the dashed vertical lines in Figure 3. However, the times of PCF disappearance are much later: 2002 February (from Lorenc et al. 2003) and 2002 April (Harvey & Recely 2002). The cessation of HL prominence eruptions was in 2002 May (see Fig. 1). Note that the three prominence-related epochs coincide with the largest peak in the SHL CME rate. If we take a careful look at the magnetic field plot in Figure 3, we see that the south polar field was close to zero around this time before assuming a steady reversal. Thus the cessation of HL activity

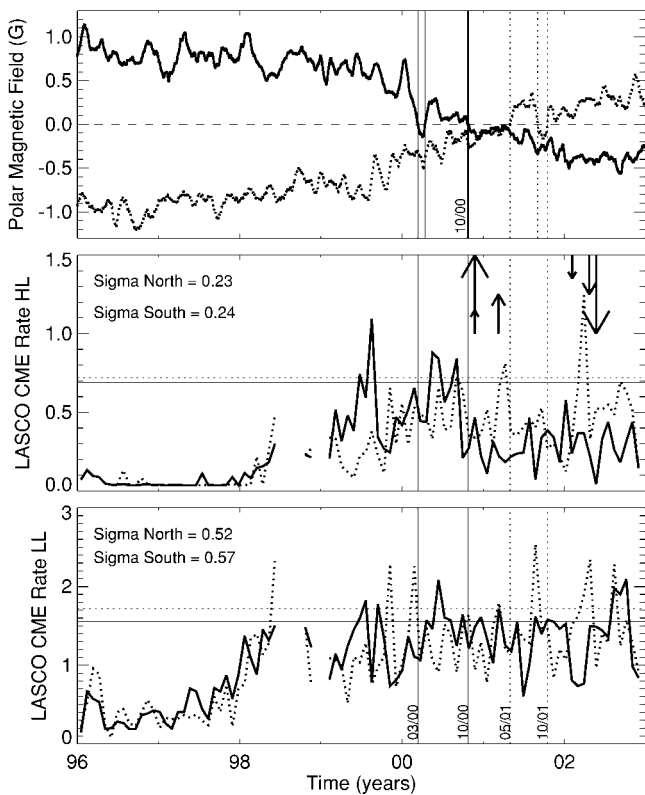


FIG. 3.—*Top*: Polar field strength averaged over regions poleward of 70° (from NSO/Kitt Peak). Times of polarity reversal are marked by the vertical lines (*solid*: north; *dashed*: south). CME rates from high (*middle*) and low latitudes (*bottom*) distinguished by the hemispheres (*solid*: north; *dotted*: south). Times when the PCF branch disappeared are marked by small (Lorenc et al. 2003) and medium (Harvey & Recely 2002) arrows. Large arrows mark the times of cessation of HL prominence eruptions from Fig. 1. The direction of the arrows indicates the hemisphere (*up*: north; *down*: south). The horizontal lines in the middle and bottom panels show the 3σ levels of the CME rates (*solid*: north; *dotted*: south). The standard deviation (σ) of the rates in the north and south are marked in the respective panels.

in the northern and southern hemispheres occurred in 2000 November and 2002 May, respectively, roughly marking the epochs of polarity reversal. The last SHL peak in Figure 3 is likely to be due to the eruptions associated with the second tier PCFs in the southern hemisphere that reached latitudes exceeding 65° as evidenced by $H\alpha$ synoptic charts (McIntosh 2003).

2.4. Comparison with Cycle 21 CME Rate

Although the observed CME rate for cycle 21 was a factor of 2 lower than the *SOHO* rate because of the poorer dynamic range of the earlier instruments, we were able to identify periods of HL CME cessation from both hemispheres. In Figure 4, we have shown the HL and LL CME rates for cycle 21 along with the NSO/Kitt Peak polar magnetic field data. Polarity reversal times from Webb et al. (1984) are also shown. The polar field was unsettled starting in the middle of 1980 all the way to the beginning of 1983, as shown by the magnetic field strength. There were corresponding “temporary” reversals indicated by the arrows from various sources. Interestingly, there were also peaks in the HL CME rates from both poles approximately at the times of these temporary reversals. The largest NHL peak for cycle 21 (toward the end of 1981) was bracketed by the disappearance of the northern PCF ac-

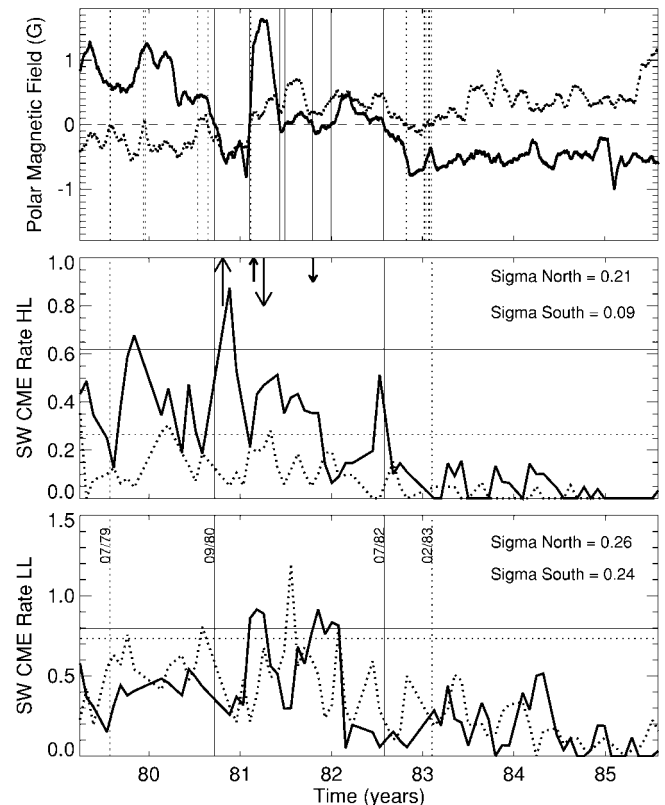


FIG. 4.—Same as Fig. 3, but for solar cycle 21. The times of PCF disappearance are also marked: small arrows as obtained from the plot in Lorenc et al. (2003) and large arrows as reported by Webb et al. (1984).

ording to Webb et al. (1984) and Lorenc et al. (2003). The first SHL CME peak was close to the south reversal (1980 September) obtained by Webb et al. (1984), while the second peak was bracketed by the disappearances of the southern PCF found in Webb et al. (1984) and Lorenc et al. (2003). There is a large spike (more than 2σ) in the NHL CME rate right at the time the north pole completely reversed around 1982 July. Note that the last period of north polar reversal listed by Webb et al. (1984) was 2002 February–March, a few months before the cessation of NHL CMEs indicated by the above NHL spike. In the south polar region, the CME rate was generally low, but there was indeed a small peak (1σ) just before the time of complete reversal in the south. Despite the fact that the CME rate data were more noisy for cycle 21, we can clearly see that the polarity reversals are marked by the cessation of HL CMEs. Webb et al. (1984) noted that the PCFs disappear months after the magnetic polar reversal. However, this is true only when the first episode of reversal is considered. The final (or complete) reversal occurs only around the time of the cessation of HL CMEs (same as PCF disappearance). The first large spike in the LL CME rates in Figure 4 occurs around the times of the PCF disappearance. This may be due to active longitudes, similar to the large spikes in the LL rates for cycle 23.

3. DISCUSSION

The results presented here bring out an important connection between the polar reversal as observed in the photospheric field and the coronal closed field as inferred from CMEs. This connection is strengthened by the fact that eruptive filaments are often found in the interiors of CMEs. We infer that the disap-

pearance of PCFs, a traditional signature used for identifying polarity reversal, is a violent process involving CMEs of mass a few times 10^{15} g and a velocity of hundreds of kilometers per second. The kinetic energy of each of these CMEs is typically a few times 10^{30} ergs. The CME process helps the closed field lines overlying PCFs, and the filaments themselves become open to complete the polarity reversal. The results presented here also support the hypothesis of Low (1997) that CMEs may represent the process by which the old magnetic flux is removed and replaced by the flux of the new magnetic cycle.

Considering the HL CMEs also provides a natural explanation for the confusion regarding the actual epoch of polarity reversal. Wang, Sheeley, & Andrews (2002) compared the time of polarity reversal in cycle 23 from source surface predictions with the time of peak HL streamer brightness (2000 February) and found them to be roughly consistent for the north pole. However, they seem to have considered the first temporary reversal (see Fig. 3, *bottom panel*). One would not expect the polarity reversal to coincide with the peak of HL streamer brightness, because the streamers would mean the presence of closed field structures near the pole (also consistent with the enhanced coronal brightness in the polar region as derived from coronal green line data; see Lorenc et al. 2003). The HL CMEs would result in the disappearance of these closed field structures before the polarity completely reverses. The polarity reversal indeed occurred toward the end of the year 2000 in the north polar region when the HL streamer brightness declined significantly (see their Fig. 4). In the south polar region, the streamer brightness did not decline significantly until the end of 2001; this is consistent with the reversal in early 2002 as indicated in our Figure 3. The decline in HL streamer brightness is therefore consistent with the involvement of HL CMEs in the polarity reversal process. The HL CMEs thus provide a mechanism by which the neutral lines that reach the poles, as

indicated by several observations including the “coronal activity waves” (Benevolenskaya, Kosovichev, & Scherrer 2002), disappear, enabling the polarity reversal. The CME involvement also provides a more complete picture than the photospheric flux-cancellation mechanism.

4. CONCLUSIONS

The primary result of this Letter is that the epochs of solar polarity reversal are closely related to the cessation of HL CME activities, including the nonsimultaneous reversal in the north and south poles. We have shown this to be true for solar cycles 21 and 23, for which complete CME data are available. Before the completion of the reversal, several temporary reversals take place with corresponding spikes in the HL CME rates. The HL CMEs also provide a natural explanation for the disappearance of closed field structures that approach the poles, which need to be removed before the reversal could be accomplished. Inclusion of CMEs along with the photospheric and subphotospheric processes completes the full set phenomena that need to be explained by any successful theory of the solar dynamo.

We thank O. C. St. Cyr for providing the Solwind CME rate data, D. Hathaway for discussion on the polar magnetic field strength, K. Shibasaki for providing the Nobeyama radioheliograph data, and T. Hoeksema for tilt angle data. We also thank the anonymous referee for helpful comments, which improved the presentation of this Letter. The NSO/Kitt Peak magnetograph data was produced cooperatively by NSF/NOAO, NASA/GSFC, and NOAA/SEC. *SOHO* is a project of international cooperation between ESA and NASA. This work was supported by NASA/LWS and NSF/SHINE (ATM 0204588) programs. A. L. thanks grant UNAM-PAPIIT IN119402 for partial support.

REFERENCES

- Benevolenskaya, E. E., Kosovichev, A. G., & Scherrer, P. H. 2002, in *Solar Variability: From Core to Outer Frontiers*, ed. A. Wilson (ESA SP-506; Noordwijk: ESA), 831
- Bilenko, I. A. 2002, *A&A*, 396, 657
- Brueckner, G. E., et al. 1995, *Sol. Phys.*, 162, 357
- Cliwer, E. W., St. Cyr, O. C., Howard, R. A., & McIntosh, P. S. 1994, in *Solar Coronal Structures*, ed. V. Rusin, P. Heinzel, & J.-C. Vial (Bratislava: VEDA), 83
- Durrant, C. J., & Wilson, P. R. 2003, *Sol. Phys.*, 214, 23
- Gopalswamy, N., Lara, A., Yashiro, S., Nunes, S., & Howard, R. A. 2003a, in *Solar Variability as an Input to the Earth's Environment*, ed. A. Wilson (ESA SP-535), in press
- Gopalswamy, N., Shimojo, M., Lu, W., Yashiro, S., Shibasaki, K., & Howard, R. A. 2003b, *ApJ*, 586, 562
- Gopalswamy, N., Yashiro, S., Nunes, S., & Howard, R. A. 2003c, *Adv. Space Res.*, in press
- Harvey, K., & Recely, F. 2002, *Sol. Phys.*, 211, 31
- Lorenc, M., Pasorek, L., & Rybanský, M. 2003, in *Solar Variability as an Input to the Earth's Environment*, ed. A. Wilson (ESA SP-535), in press
- Low, B. C. 1997, *Geophys. Monogr.*, 99, 39
- Makarov, V. I., Tlatov, A. G., & Sivaraman, K. R. 2001, *Sol. Phys.*, 202, 11
- McIntosh, P. E. 2003, in *Solar Variability as an Input to the Earth's Environment*, ed. A. Wilson (ESA SP-535), in press
- Wagner, W. J. 1986, in *Coronal and Prominence Plasmas*, ed. A. I. Poland (NASA CP-2442; Washington, DC: NASA), 215
- Waldmeier, M. 1960, *Zeitschrift für Astrophys.*, 49, 176
- Wang, Y.-M., Sheeley, N. R., & Andrews, M. D. 2002, *J. Geophys. Res.*, 107, 10
- Webb, D. F., Davis, J. M., & McIntosh, P. S. 1984, *Sol. Phys.*, 92, 109